2019 19th International Conference on Control, Automation and Systems (ICCAS 2019)
Oct. 15~18, 2019; ICC Jeju, Jeju, Korea

Homogeneous Quantitative Measure of Caging Grasps with both Geometrical and Mechanical Constraints

Satoshi Makita[1*] and Koshi Makihara[2]

[1]Dept. of Control Engineering, National Institute of Technology, Sasebo College,
Sasebo, 8571193, Japan (makita@sasebo.ac.jp), * Corresponding author
[2]Graduate School of Systems and Information Engineering, Tsukuba University,
Tsukuba, 3058573, Japan (makihara@ms.esys.tsukuba.ac.jp)

Abstract: This paper presents a homogeneous evaluation of difficulty of moving attributed to both geometrical and mechanical constraints. Although caging grasp usually considers to confine an object geometrically by surrounding robots, it is not always feasible due to limitation of robots such as few number of robots or fingers. Such incomplete caging is often called as partial caging, and in which the object can escape from the cage of robots. And then the object is prevented from moving by both geometrical constraints and mechanical effects. The former can be discussed with arrangements of robots and environments, and the latter is investigated with static/dynamic analyses of contact forces. This paper addresses both different indexes homogeneously based on robustness measure for grasping and contact tasks. We introduce a novel interpretation for evaluation of complete/partial caging quality, and show some numerical examples.

Keywords: Manipulation, Grasping, Caging, Force analysis

1. INTRODUCTION

Caging grasp considering geometrical constraints has been an attractive research field in a couple of decades, which is substitute for or complement to conventional grasping and manipulation based on mechanical analyses [1]. Position-controlled robots usually surround an object to avoid it from escaping the *cage*, and transport it by keeping the robots' formation. A caging problem in robotics was firstly introduced by Rimon and Blake [2], [3] for immobilizing grasps by a two-fingered hand. Later various types of caging have been widely studies such as three-fingered caging [4], caging by multiple mobile robots [5]. On the other hand, *complete* caging ensuring geometrical constraint for the captured object is not sometimes accomplished due to limitation of robots, such as few robots. Thus *partial* caging where the object has escape paths through gaps between robots should be contemplated to benefit geometrical constraints in grasping. Makapunyo et al. measure partial cage quality as difficulty of motion planning of objects to escape from the incomplete cage [6], by using probabilistic search algorithms [7]. This approach focuses on fully geometrical problems and is applicable even to complicated situations in higher dimensional space. On the other hand, under gravitational fields, an object needs some potential energy to escape from the cage with opposing the gravitational forces [8]. It can be applied to placing objects at partially fenced place [9].

Our approach to evaluate partial cage quality depending on both geometrical and mechanical constraints is based on the static analysis of contact forces in grasping and manipulation [10]. The mechanical analysis derives a robustness index against external wrenches applied to the object during manipulation. Our proposed index of caging quality is expressed as difficulty to move in the cage. When some obstacles such as position-controlled robots exist, the object never move toward the obstacles due to geometrical constraints. When the object has feasible motion but some external wrenches such as gravitational force prevent it from beginning of the motion, the object seems to be restricted to move by mechanical constraints. In this manner, we homogeneously evaluate quality of both partial and complete caging.

This work was supported by JSPS KAKENHI JP17H04669.

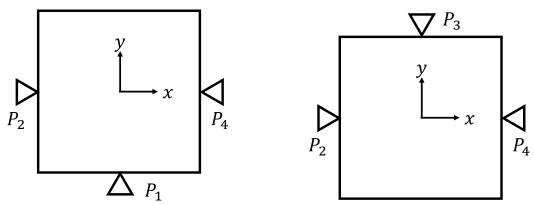

(a)Arrange a finger to oppose to the gravitational force

(b)No fingers support the bottom of the object

Fig. 1 Grasping by three-fingered hand in two-dimensional space. Gravitational force is applied toward $-y$ direction.

Note that motion of objects in this paper is only Euclidean motion [11], each of which is regarded as a single rotational motion around an arbitrary point. Hence complicated and winding motion are often out of scope.

Let consider three-fingered grasp as Fig. 1, where the gravitational force is applied toward $-y$ direction. Our proposed algorithm evaluates each robustness of grasping, and then arrangement of fingers in Fig. 1(a) has higher robustness. The grasped object in Fig. 1(b) tends to naturally go out from the hand. In contrast, the object in Fig. 1(a) requires necessary potential energy to escape from the hand through the gap above the object. Both objects never move horizontally because of presence of fingers unless excessive external wrenches defeat joint torques. If the fingers are in position control and are equivalent to rigid environments, we need infinite external wrenches.

2. MECHANICAL MODEL

The mechanical model in this paper refers to the previous studies [10], [12], and is briefly summarized with principal formulas. The following formulation is discussed as problems in three-dimensional space, and it is easily applied to those in two-dimensional space.

2.1 Assumptions and Notations

Firstly we assume that all the objects and robots are in static, thus quasi-static and dynamic movement are not considered. In addition, all the objects, robots, and environments are composed of rigid bodies. Then Coulomb friction at all the contact points between those bodies are applied, and each friction cone can be approximated by a convex n-polygonal pyramid. As for the static frictional forces, combinations of those directions are limited due to feasible motion of rigid bodies [10] (See (7)). In the studies on robotic caging, all the robots or robotic fingers are assumed to be in position-controlled because caging is a problem how to surround objects by robots to prevent the object from escaping from "the cage". However position-controlled robots often cause excessive internal forces in tasks with contacts such as grasping. In order to avoid that unacceptable results, we adopt position/force hybrid control to all the fingers for CONVENIENCE. Each hybrid-controlled finger with a prismatic joint can actively control the force in a certain direction, and it can be regarded as a finger of parallel jaw gripper.

The following notations are defined.

- N : the number of fingers.
- M_i : the number of contact points on the i-th finger.
- $M = \sum_{i=1}^{N} M_i$: the amount of contact points.
- $L_i = 1$: the number of joints in the i-th finger.
- $L := \sum_{i=1}^{N} L_i = N$: the amount of joints.
- P_{ik} : the k-th contact point on the i-th finger. Every contact point is numbered in order from the base of each finger.
- P_l : the l-th contact points in all the contact points. Then $l = \sum_{n=1}^{i-1} L_n + k$.
- $\boldsymbol{p}_l \in \mathbb{R}^3$: the position vector of the contact point, P_l.
- $\boldsymbol{t}_{i1},\ \boldsymbol{t}_{i2} \in \mathbb{R}^3$: the tangential vectors that are orthogonal vectors spanning a corresponding tangential plane at the l-th contact point.
- $\boldsymbol{n}_l \in \mathbb{R}^3$: the unit normal vector at the l-th contact point toward inside of the object.

Additionally the following mathematical expressions are used.

- Diagonal matrix or block diagonal matrix:

$$\mathrm{diag}\,(\boldsymbol{A}_1, \ldots, \boldsymbol{A}_n) := \begin{bmatrix} \boldsymbol{A}_1 & & \boldsymbol{O} \\ & \ddots & \\ \boldsymbol{O} & & \boldsymbol{A}_n \end{bmatrix}$$

- Inequality between two vectors: $\boldsymbol{a} := [a_1, \ldots, a_n]^T$, $\boldsymbol{b} := [b_1, \ldots, b_n]^T$ are defined. If $\boldsymbol{a} > \boldsymbol{b}$, then $a_i > b_i \ (i = 1, \ldots, n)$.

2.2 Contact Forces

The contact force, $\boldsymbol{f}_l \in \mathbb{R}^3$, which is applied to the object at the contact point, P_l is expressed as:

$$\boldsymbol{f}_l = \boldsymbol{C}_l \boldsymbol{k}_l, \tag{1}$$

where $\boldsymbol{C}_l := [\boldsymbol{c}_{l1} \ldots \boldsymbol{c}_{lr_l}] \in \mathbb{R}^{3\times r_l}$. $\boldsymbol{c}_{lm}$ denotes the m-th unit edge vector of the convex n-gonal pyramid approximating the friction cone at the contact point, P_l. $\boldsymbol{k}_l := [k_{k1}, \ldots, k_{lr_l}]^T \in \mathbb{R}^{r_l}$ is a vector corresponding the magnitude of the contact force, $\boldsymbol{f}_l$, and $\boldsymbol{k}_l \geq \boldsymbol{0} = [0, \ldots, 0]^T$.

The contact force, $\boldsymbol{f}_{ik}$, applied at the contact point, P_{ik} is related to the joint torques of i-th finger as:

$$\boldsymbol{J}_{ik}^T \boldsymbol{f}_{ik} = \boldsymbol{\tau}_i = [\tau_{i1} \ldots, \tau_{iL_i}]^T \in \mathbb{R}^{L_i}, \tag{2}$$

where $\boldsymbol{J}_{ik} \in \mathbb{R}^{3\times L_i}$ denotes the Jacobian matrix for the contact point, P_{ik}, and $\tau_{ij} \in \mathbb{R}^1$ denotes the j-th joint's torque of the i-th finger. From the assumption in this chapter, every finger is in hybrid control, and it is equal to a prismatic joint with 1 degree of freedom. Thus,

$$\boldsymbol{J}_{ik} = \boldsymbol{m}_i \in \mathbb{R}^3, \tag{3}$$

$$\boldsymbol{\tau}_i = \tau_{i1} \in \mathbb{R}^1, \tag{4}$$

where $\boldsymbol{m}_i$ denotes a unit vector along the direction of joint motion of the i-th finger. Additionally a finger can be in position-controlled if $\tau_{i1} = +\infty$.

The following matrices are defined.

$$\boldsymbol{W} := \begin{bmatrix} \boldsymbol{I}_3 & \ldots & \boldsymbol{I}_3 \\ \boldsymbol{p}_1 \times \boldsymbol{I}_3 & \ldots & \boldsymbol{p}_1 \times \boldsymbol{I}_3 \end{bmatrix} \in \mathbb{R}^{6\times 3M},$$
$$\boldsymbol{C} := \mathrm{diag}\,(\boldsymbol{C}_1, \ldots, \boldsymbol{C}_M) \in \mathbb{R}^{3M\times r},$$
$$\boldsymbol{k} := \left[\boldsymbol{k}_1^T, \ldots, \boldsymbol{k}_M^T\right]^T \in \mathbb{R}^r,$$
$$\boldsymbol{T} := \mathrm{diag}\,(\boldsymbol{T}_1, \ldots, \boldsymbol{T}_M) \in \mathbb{R}^{3M\times 2M},$$
$$\boldsymbol{T}_l := \begin{bmatrix} \boldsymbol{t}_{l1} & \boldsymbol{t}_{l2} \end{bmatrix} \in \mathbb{R}^{3\times 2},$$
$$\boldsymbol{J} := \mathrm{diag}\,(\boldsymbol{J}_1, \ldots, \boldsymbol{J}_N) \in \mathbb{R}^{3M\times L},$$
$$\boldsymbol{J}_i := \left[\boldsymbol{J}_{i1}^T, \ldots, \boldsymbol{J}_{iM_i}^T\right]^T \in \mathbb{R}^{3M_i\times L_i},$$
$$\boldsymbol{f} := \left[\boldsymbol{f}_1^T, \ldots, \boldsymbol{f}_M^T\right]^T \in \mathbb{R}^{3M},$$
$$\boldsymbol{\tau} := \left[\boldsymbol{\tau}_1^T, \ldots, \boldsymbol{\tau}_N^T\right]^T \in \mathbb{R}^L,$$

where $\boldsymbol{I}_n$ denotes an identity matrix with dimension of $n\times n$. $\boldsymbol{p}\times\boldsymbol{I}_3$ denotes a skew matrix, and then $(\boldsymbol{p}_l \times \boldsymbol{I}_3)\,\boldsymbol{x} = \boldsymbol{p}_l \times \boldsymbol{x}$.

With the notations, all the contact forces, $\boldsymbol{f}$ can be expressed as follows:

$$\boldsymbol{f} = \boldsymbol{C}\boldsymbol{k}. \tag{5}$$

Thus frictional forces at contact points are expressed as:

$$\boldsymbol{T}^T \boldsymbol{f} = \boldsymbol{T}^T \boldsymbol{C}\boldsymbol{k} \in \mathbb{R}^{2M}. \tag{6}$$

It is reported in [10] that the static frictional forces occur under the limitation of their combination. The constraint on static friction has been originally derived by Omata et al. [13], [14], taking feasible motion of rigid bodies into consideration. With the constraint, every feasible combination of static frictional forces must satisfy the following conditions:

$$\boldsymbol{S}\boldsymbol{T}^T\boldsymbol{C}\boldsymbol{k} \leq \boldsymbol{0}, \tag{7}$$

$$\boldsymbol{T}^T\left(\boldsymbol{I}_{3M} - \boldsymbol{B}\right)\boldsymbol{C}\boldsymbol{k} = \boldsymbol{0}. \tag{8}$$

$\boldsymbol{S} := \mathrm{diag}\left(s_{11}, s_{12}, s_{21}, s_{22}, \ldots, s_{M1}, s_{M2}\right) \in \mathbb{R}^{2M\times 2M}$ denotes signs for direction of infinitesimal displacement, which is equivalent to shear strain of contact point, and $s_{lm} = \{\pm 1, 0\}$. As Coulomb's friction law, the infinitesimal displacement seems to cause static friction [15]. $\boldsymbol{B} := \mathrm{diag}\left(b_1\boldsymbol{I}_3, \ldots, b_M\boldsymbol{I}_3\right) \in \mathbb{R}^{3M\times 3M}$ is a selection matrix that determines whether each infinitesimal displacement occurs at the corresponding contact points. In analysis of indeterminate forces in grasping and contact tasks, direction of external wrench as disturbances can be arbitrarily considered. When the external wrench causes infinitesimal motion of the target object, each resultant infinitesimal displacement occurs at the contact point. If the displacement occurs at the contact point, P_l, then $b_l = 1$. Otherwise $b_l = 0$. Thus $s_{lm} = 0$ whenever $b_l = 0$. (7) expresses that the direction of the infinitesimal displacement at the contact point is opposite to the corresponding tangential force. (8) expresses that there are no frictional forces at the contact points without any infinitesimal displacement. The following linear programming problem judges whether the combination of the infinitesimal displacement is feasible or not:

$$\underset{\boldsymbol{q},\boldsymbol{V},\dot{\boldsymbol{\theta}}}{\text{maximize}}\ \boldsymbol{1}^T\boldsymbol{q}$$

$$\text{subject to} \begin{cases} \boldsymbol{B}\begin{bmatrix}\boldsymbol{W}^T & \boldsymbol{J}\end{bmatrix}\begin{bmatrix}\boldsymbol{V} \\ -\dot{\boldsymbol{\theta}}\end{bmatrix} = \boldsymbol{T}\boldsymbol{S}\boldsymbol{q} \\ \boldsymbol{q} \geq \boldsymbol{1} \end{cases}, \tag{9}$$

where $\boldsymbol{V} \in \mathbb{R}^6$ denotes the velocity of the object with rigid body, $\dot{\boldsymbol{\theta}} \in \mathbb{R}^L$ denotes the joint angular velocity of robots, and $\boldsymbol{1} = [1, \ldots, 1]$. If $\boldsymbol{q}$ ($> \boldsymbol{0}$) satisfying (9), the objective function diverges to infinity.

The relationship between contact forces and joint torques can be expressed as:

$$\boldsymbol{J}^T\boldsymbol{f} = \boldsymbol{J}^T\boldsymbol{C}\boldsymbol{k} = \boldsymbol{\tau}. \tag{10}$$

Force equilibrium for the object can be expressed as:

$$\boldsymbol{W}\boldsymbol{f} = \boldsymbol{W}\boldsymbol{C}\boldsymbol{k} = -\left(\boldsymbol{Q}_{\text{known}} + \boldsymbol{Q}_{\text{dist}}\right), \tag{11}$$

where $\boldsymbol{Q}_{\text{known}} \in \mathbb{R}^6$ denotes known external wrenches such as the gravitational force, and $\boldsymbol{Q}_{\text{dist}} \in \mathbb{R}^6$ denotes unknown external disturbances.

2.3 Robustness Measure

Maeda et al. presented a measurement method of robustness for grasping and contact tasks [16]. The objective value is equal to the minimum external wrench that precludes manipulation, and it can be calculated for arbitrary direction of disturbances. In this paper, the value of robustness, z is calculated by the following series of minimax problems.

$$z = \min_i z_i, \tag{12}$$

$$z_i = \max_{\zeta,\boldsymbol{k},\boldsymbol{B},\boldsymbol{S},\boldsymbol{\tau}} \zeta, \tag{13}$$

$$\text{subject to} \begin{cases} \zeta\left(\boldsymbol{R}^{\frac{1}{2}}\right)^{-1}\boldsymbol{l}_i + \boldsymbol{Q}_{\text{known}} + \boldsymbol{W}\boldsymbol{C}\boldsymbol{k} = \boldsymbol{0} \\ \boldsymbol{J}^T\boldsymbol{C}\boldsymbol{k} - \boldsymbol{\tau} = \boldsymbol{0} \\ \boldsymbol{T}^T\left(\boldsymbol{I}_{3M} - \boldsymbol{B}\right)\boldsymbol{C}\boldsymbol{k} = \boldsymbol{0} \\ \boldsymbol{S}\boldsymbol{T}^T\boldsymbol{C}\boldsymbol{k} \leq \boldsymbol{0} \\ \boldsymbol{0} \leq \boldsymbol{\tau} \leq \tau_{\max}\boldsymbol{1} \\ \boldsymbol{k} \geq \boldsymbol{0} \\ \zeta \geq 0 \end{cases},$$

where $\tau_{\max}$ denotes the maximum value of joint torque. $\boldsymbol{R}^{\frac{1}{2}} \in \mathbb{R}^{6\times 6}$ is the Cholesky decomposition of $\boldsymbol{R}$. We define a scaling matrix $\boldsymbol{R} := \begin{bmatrix}\boldsymbol{I}_3 & \boldsymbol{O} \\ \boldsymbol{O} & M_0\boldsymbol{J}_0^{-1}\end{bmatrix}$ with the mass of the object, M_0 and the inertia tensor of the object for the center of mass, $\boldsymbol{J}_0$, in order to have a coordinate-invariant norm.

$\boldsymbol{l}_i \in \mathbb{R}^6$ denotes the direction of external wrench, $\boldsymbol{Q}_{\text{dist}}$. With (13), we evaluate the robustness of the manipulated object against a certain external disturbance whose direction is determined by $\boldsymbol{l}_i$.

3. MEASUREMENT OF CAGING QUALITY BASED ON ROBUSTNESS ANALYSIS

With the robustness of the manipulated object derived by (12) and (13), we quantitatively evaluate quality of both complete and partial caging grasps. The robustness means the difficulty of movement for the object, and also it leads the difficulty of escaping from the complete/partial cage for the captured object. Note that position and force hybrid control is adopted for all the fingers instead of position-control in order to avoid excessive internal forces applied to the object. In general, position control for robot fingers is firstly considered because geometrical arrangements of the fingers to capture the object is an essential problem of caging grasps. On the other hand, as for static analyses, contacts with position-controlled fingers often cause excessive internal forces. For convenience to avoid such undesirable results, hybrid-controlled fingers have bounded joint torques.

When an external disturbance as six-dimensional wrench is applied to a grasped object, the object remains its manipulation state to some extent thanks to contact forces applied by robots and the gravitational force. If the maximum external wrench, which is equal to the evaluated robustness, is applied to the object, the object will begin to move because force equilibrium for the object breaks. Therefore the robustness for grasping and manipulation for a certain direction represents difficulty of moving toward the direction. Note that the motion of the object at that time can be regarded as Euclidean motion, that is, be approximated by a single rotational motion.

For example as Fig. 1, the grasped object cannot move toward the direction where any robotic fingers exist such as $+x$-direction unless an external wrench applied to the object breaks force equilibrium. Thus toward position-controlled robots, which can be equivalent to rigid environments, the object cannot move. In this manner, we can judge a captured object is geometrically constrained by surrounding robots when the calculated robustness for the corresponding direction reaches its upper bound.

As for direction toward which the captured object can escape, known external forces such as the gravitational force and contact forces applied by robots interfere with the object to move. Thus the calculated robustness represents difficulty to move toward the direction.

4. NUMERICAL EXAMPLES

Some numerical simulations verify our proposed method to evaluate quantitatively quality of complete/partial caging grasps. Homogeneous measure for both geometrical and mechanical constraints can be calculated based on the robustness analysis for grasping and contact tasks. Both two and three dimensional situations appear in this section.

It is assumed that the mass of target object is 1 ($M_0 = 1$), and mass distribution is uniform. The coefficient of static friction is 0.3. The upper bound of torque for hybrid fingers $\tau_{\max} = 40.0$.

4.1 Caging Grasp in Two Dimensional Space

We set the vector $\boldsymbol{l}_i$, which denotes the direction of external wrench, as following 14 patterns: $\boldsymbol{l}_i = [\pm1, 0, 0]^T, [0, \pm1, 0]^T, [0, 0, \pm1]^T, \frac{1}{\sqrt{3}}[\pm1, \pm1, \pm1]^T$. A known wrench including the gravitational force is $\boldsymbol{Q}_{\text{known}} = [0, -9.8, 0]^T$.

4.1.1 For a Square Object with Multiple Fingers

Considering cases that multiple pointed fingers grasp a square object as shown in Fig. 1 and 2, we compare each robustness of grasping. Firstly four fingers are arranged one by one for every edge as Fig. 2(e), and numbered as $P_1, \ldots, P_4$. Thus each finger has a contact point with an edge. This case seems to be *Complete* caging (or form closure), where the captured object cannot escape from the cage of fingers. After that we reduce contact points and evaluate robustness for each grasp. The parameters for calculation are as follows:

$$\boldsymbol{p}_1 = \begin{bmatrix} 0.0 \\ -1.0 \end{bmatrix}, \quad \boldsymbol{p}_2 = \begin{bmatrix} -1.0 \\ 0.0 \end{bmatrix}, \quad \boldsymbol{p}_3 = \begin{bmatrix} 0.0 \\ 1.0 \end{bmatrix}, \quad \boldsymbol{p}_4 = \begin{bmatrix} 1.0 \\ 0.0 \end{bmatrix},$$
$$\boldsymbol{T}_1 = \begin{bmatrix} 1 \\ 0 \end{bmatrix}, \quad \boldsymbol{T}_2 = \begin{bmatrix} 0 \\ 1 \end{bmatrix}, \quad \boldsymbol{T}_3 = \begin{bmatrix} 1 \\ 0 \end{bmatrix}, \quad \boldsymbol{T}_4 = \begin{bmatrix} 0 \\ 1 \end{bmatrix},$$
$$\boldsymbol{N}_1 = \begin{bmatrix} 0 \\ 1 \end{bmatrix}, \quad \boldsymbol{N}_2 = \begin{bmatrix} 1 \\ 0 \end{bmatrix}, \quad \boldsymbol{N}_3 = \begin{bmatrix} 0 \\ -1 \end{bmatrix}, \quad \boldsymbol{N}_4 = \begin{bmatrix} -1 \\ 0 \end{bmatrix},$$
$$\boldsymbol{J}_1 = \boldsymbol{N}_1, \quad \boldsymbol{J}_2 = \boldsymbol{N}_2, \quad \boldsymbol{J}_3 = \boldsymbol{N}_3, \quad \boldsymbol{J}_4 = \boldsymbol{N}_4.$$

Every calculated robustness is shown in Table 1. Comparing two pinching grasps (Fig. 2(a) and 2(b)), the case of pinching vertically marks higher robustness than pinching horizontally. This result seems to be intuitive because the finger arranged on the bottom of the object opposes to the gravitational force.

Table 1 Robustness of each grasp patterns

Fig. 1(a): Without contacts on the top	24.23
Fig. 1(b): Without contacts on the bottom	10.17
Fig. 2(a): Pinching the object horizontally	10.17
Fig. 2(b): Pinching the object vertically	12.99
Fig. 2(c): Without contacts on the left side	12.99
Fig. 2(d): Without contacts on the right side	12.99
Fig. 2(e): Complete caging	52.16

As for grasping by three fingers, the arrangement of fingers without contacts on the top of the object (Fig. 1(a)) marks highest robustness, comparing with other cases (Fig. 2(c) and Fig. 2(d)). The reason of these results is similar to the above.

Naturally, the case of Fig. 2(e) where the object is completely surrounded with contacts on all the edges marks the highest robustness in these simulation results. Since this arrangement of fingers satisfy the conditions of complete caging, the measured robustness diverges to infinity if all the fingers are in position-controlled.

Although the robustness reflects the quality of caging grasps that depends on difficulty of movement attributed to both geometrical and mechanical constraints, the minimum value of the objective function is not sufficient. As for Fig. 1(b) and 2(a), these two cases have the same minimum value of robustness. Nevertheless it is intuitively seemed the difficulty of movement for the grasped object is higher in the case of Fig. 1(b). To investigate these details, we add up robustness values for every direction of external wrench, $\boldsymbol{l}_i$. The amount of robustness values in Fig. 1(b) is 404.6, and that of Fig. 2(a) is 290.5. Thus the quality of geometrical constraint depending on arrangement of fingers can be evaluated by the amount of robustness for every direction. Note that more direction of $\boldsymbol{l}_i$ obviously enable more precise analyses. In this paper, it is assumed that fourteen directions of external wrench is enough to analyze such characteristic trend of robustness.

4.1.2 Pinching a T-shaped Object

Consider pinching grasp for a T-shaped object by a parallel jaw gripper. Numbering of contact points are shown in Fig. 3, and common parameters for calculation are as follows: $\tau_{\max} = 40.0$,

$$\boldsymbol{J}_{11} = \begin{bmatrix} -1.0 \\ 0.0 \end{bmatrix}, \ \boldsymbol{J}_{12} = \begin{bmatrix} -1.0 \\ 0.0 \end{bmatrix}, \ \boldsymbol{J}_{21} = \begin{bmatrix} 1.0 \\ 0.0 \end{bmatrix}, \ \boldsymbol{J}_{22} = \begin{bmatrix} 1.0 \\ 0.0 \end{bmatrix}.$$

As for the case of Fig. 3(a),

$$\boldsymbol{p}_{11} = \boldsymbol{p}_1 = \begin{bmatrix} 1.0 \\ 0.075 \end{bmatrix}, \ \boldsymbol{p}_{12} = \boldsymbol{p}_2 = \begin{bmatrix} 1.075 \\ 0.0 \end{bmatrix},$$
$$\boldsymbol{p}_{21} = \boldsymbol{p}_3 = \begin{bmatrix} -1.0 \\ 0.075 \end{bmatrix}, \ \boldsymbol{p}_{22} = \boldsymbol{p}_4 = \begin{bmatrix} -1.075 \\ 0.0 \end{bmatrix},$$
$$\boldsymbol{T}_1 = \begin{bmatrix} 0 \\ 1 \end{bmatrix}, \ \boldsymbol{T}_2 = \begin{bmatrix} 1 \\ 0 \end{bmatrix}, \ \boldsymbol{T}_3 = \begin{bmatrix} 0 \\ 1 \end{bmatrix}, \ \boldsymbol{T}_4 = \begin{bmatrix} 1 \\ 0 \end{bmatrix},$$
$$\boldsymbol{N}_1 = \begin{bmatrix} -1 \\ 0 \end{bmatrix}, \ \boldsymbol{N}_2 = \begin{bmatrix} 0 \\ -1 \end{bmatrix}, \ \boldsymbol{N}_3 = \begin{bmatrix} 1 \\ 0 \end{bmatrix}, \ \boldsymbol{N}_4 = \begin{bmatrix} 0 \\ -1 \end{bmatrix}.$$

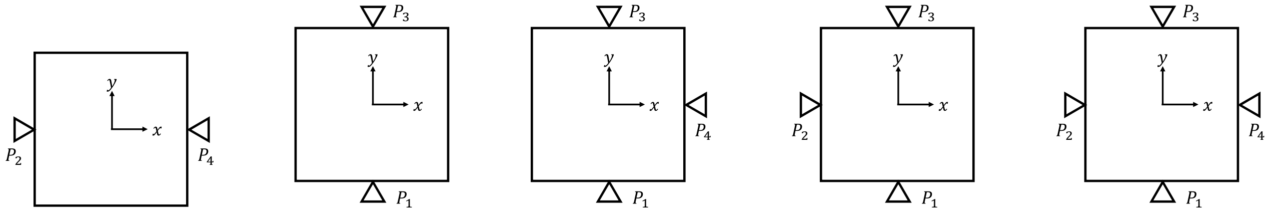

(a)Pinching by two fingers, whose location is parallel to x-axis.

(b)Pinching by two fingers, whose location is parallel to y-axis.

(c)Grasping by three fingers without contact points on the left side of the object

(d)Grasping by three fingers without contact points on the right side of the object

(e)Complete caging by four fingers

Fig. 2 Grasping a square object

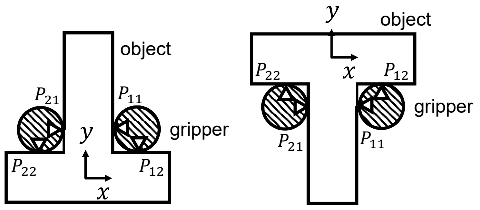

(a)Pinching an upside-down object

(b)pinching with support by the gripper

Fig. 3 Grasping a t-shaped object

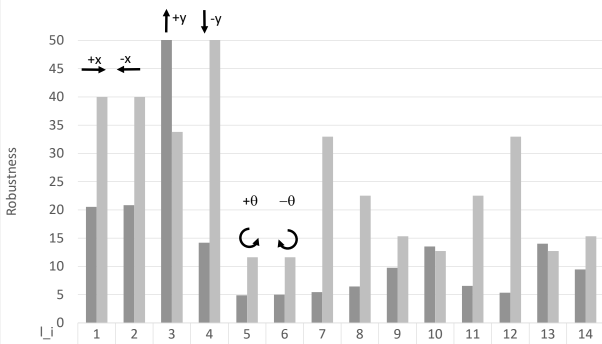

l_i	1	2	3	4	5	6	7	8	9	10	11	12	13	14
Fig. 3(a)	20.54	20.83	1E+06	14.2	4.883	5.005	5.443	6.444	9.765	13.54	6.55	5.347	14.01	9.461
Fig. 3(b)	40	40	33.8	1E+06	11.62	11.62	32.96	22.52	15.34	12.73	22.52	32.96	12.73	15.34

Fig. 4 Simulation result of calculated robustness for pinching a t-shaped object in 2D

As for the case of Fig. 3(b),

$$\boldsymbol{p}_{11} = \boldsymbol{p}_1 = \begin{bmatrix} 1.0 \\ -0.075 \end{bmatrix},\ \boldsymbol{p}_{12} = \boldsymbol{p}_2 = \begin{bmatrix} 1.075 \\ 0.0 \end{bmatrix},$$
$$\boldsymbol{p}_{21} = \boldsymbol{p}_3 = \begin{bmatrix} -1.0 \\ -0.075 \end{bmatrix},\ \boldsymbol{p}_{22} = \boldsymbol{p}_4 = \begin{bmatrix} -1.075 \\ 0.0 \end{bmatrix},$$
$$\boldsymbol{T}_1 = \begin{bmatrix} 0 \\ 1 \end{bmatrix},\ \boldsymbol{T}_2 = \begin{bmatrix} 1 \\ 0 \end{bmatrix},\ \boldsymbol{T}_3 = \begin{bmatrix} 0 \\ 1 \end{bmatrix},\ \boldsymbol{T}_4 = \begin{bmatrix} 1 \\ 0 \end{bmatrix},$$
$$\boldsymbol{N}_1 = \begin{bmatrix} -1 \\ 0 \end{bmatrix},\ \boldsymbol{N}_2 = \begin{bmatrix} 0 \\ 1 \end{bmatrix},\ \boldsymbol{N}_3 = \begin{bmatrix} 1 \\ 0 \end{bmatrix},\ \boldsymbol{N}_4 = \begin{bmatrix} 0 \\ 1 \end{bmatrix}.$$

The calculated results of robustness against each direction of external wrench are shown in Fig. 4. The minimum robustness values of Fig. 3(a) and Fig. 3(b) are 6.42 and 15.08 respectively. Moreover Fig. 4 illustrates that robustness values for each direction of external wrench. The robustness for the direction of $+y$ ($\boldsymbol{l}_3$) in Fig. 3(a) and that for the direction of $-y$ ($\boldsymbol{l}_4$) in Fig. 3(b) diverge to infinity because the fingers are in position control for each corresponding direction, where the contact points, P_{12} and P_{22}, exist. Hence we exclude these diverged values when amount of robustness values is calculated. Each calculated amount for Fig. 3(a) and Fig. 3(b) is 181.7 and 402.4 respectively. These results also suggest that arrangement of position-controlled fingers to support such as gravitational force contributes to more robust grasps, even regardless of conventional force/form closure.

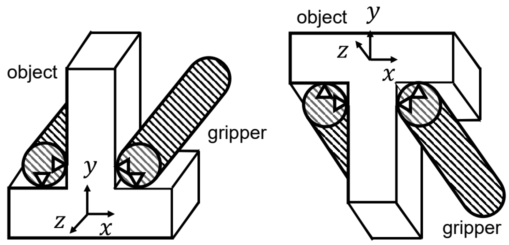

(a)Pinching an upside-down object

(b)pinching with support by the gripper

Fig. 5 Grasping a t-shaped object

4.2 Caging Grasp in Three Dimensional Space

Consider pinching grasp for a T-shaped object by a parallel jaw gripper in three dimensional space as Fig. 5. We set the vector $\boldsymbol{l}_i$, which denotes the direction of external wrench, as following 76 patterns: $\boldsymbol{l}_i = [\pm1, 0, 0, 0, 0, 0]^T, [0, \pm1, 0, 0, 0, 0]^T, [0, 0, \pm1, 0, 0, 0]^T, [0, 0, 0, \pm1, 0, 0]^T, [0, 0, 0, 0, \pm1, 0]^T, [0, 0, 0, 0, 0, \pm1]^T, \frac{1}{\sqrt{6}}[\pm1, \pm1, \pm1, \pm1, \pm1, \pm1]^T$. A known wrench including the gravitational force is $\boldsymbol{Q}_{\text{known}} = [0, -9.8, 0, 0, 0, 0]^T$. Each position of contact point and its normal vector are set similarly to Sec. 4.1.2, where each finger has four contact points.

The calculated results of robustness against each direction of external wrench are shown in Fig. 6. The minimum robustness values of Fig. 5(a) and Fig. 5(b) are 4.57 and 10.87 respectively. These results are naturally similar to the results shown in Sec. 4.1.2.

5. DISCUSSION

In this paper, we propose a homogeneous quantitative measure of caging grasps that depend on geometrical and mechanical constraints, and demonstrate numerical simulations in both two and three dimensional spaces.

As for a square object in 2D scene, the results shown in Table 1 address that minimum robustness values are same between pinching a square object(Fig. 2(a)) and pinching a square object with additional contact point on the top of the object (Fig. 1(b)). In contrast, the additional contact point contributes to higher robustness for external disturbances in the direction of $+y$. Thus arrangement

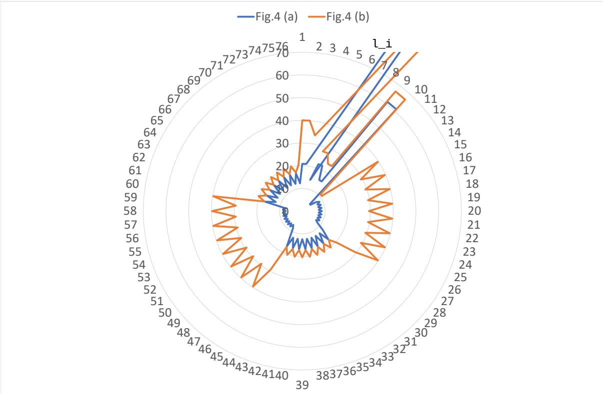

Fig. 6 Simulation result of calculated robustness for pinching a t-shaped object in 3D

of fingers on the top of the object has low priority. Similarly with comparing cases of Fig. 2(b), Fig. 2(c), and Fig. 2(d), every minimum robustness value is same. Thus prior arrangement of fingers for robust grasps is to locate a finger (or fingers) on the bottom of the object to oppose to gravitational force. This result is quite intuitive, and the located fingers can be even in position-controlled, which is then equivalent to rigid environments. The cases as Fig. 1(a) can be called as "gravity caging" [9].

As for pinching T-shaped object shown in Fig. 3, a difference of robustness values depends only on posture of the grasped object. In Fig. 3(b), the fingers support the object passively to oppose the gravitational force in $-y$ direction. Even if the fingers slip and lose contact forces applied to the object, the object remains under constraint by fingers. Therefore arrangement of fingers for geometrical constraint should be additionally taken into consideration. It can contribute to reliable grasping and manipulation regardless of force closure.

6. CONCLUSIONS

This paper presents a novel quantitative measure of caging grasps, in which both geometrical and mechanical constraints are homogeneously treated. In partial caging, surrounding an object by robots is not complete, and then the object can escape from the surrounding cage, although in contrast, complete caging can avoid rigorously the object from escaping. Then arrangement of fingers restricts the object's motion geometrically, and also mechanical effects such as the gravitational force prevent the object from moving toward its opposite direction. Our proposed measurement based on analyses of robustness in grasping and manipulation merges both these difficulty of moving and fairly evaluates. Some numerical examples for two and three dimensional scenes are presented as applications of our method.

In future works, the evaluation of partial cage quality will be used in motion planning for grasping and manipulation because such geometrical constraint can contribute to reliable tasks even when force closure breaks.

REFERENCES

[1] S. Makita and W. Wan, "A survey of robotic caging and its applications," *Advanced Robotics*, 31, 19-20, 1071–1085, 2017.

[2] E. Rimon and A. Blake, "Caging 2d bodies by 1-parameter two-fingered gripping systems," in *Proc. of IEEE Int. Conf. on Robotics and Automation*, 1996, 1458–1464.

[3] ——, "Caging planar bodies by one-parameter two-fingered gripping systems," *Int. J. of Robotics Research*, 18, 3, 299–318, 1999.

[4] J. Erickson, et al., "Capturing a convex object with three discs," *IEEE Trans. on Robotics*, 23, 6, 1133–1140, 2007.

[5] Z. Wang and V. Kumar, "Object closure and manipulation by multiple cooperating mobile robots," in *Proc. of IEEE Int. Conf. on Robotics and Automation*, 2002, 394–399.

[6] T. Makapunyo, et al., "Measurement framework of partial cage quality," in *Proc. of IEEE Int. Conf. on Robotics and Biomimetics*, 2012, 1812–1816.

[7] ——, "Measurement framework of partial cage quality based on probabilistic motion planning," in *Proc. of IEEE Int. Conf. on Robotics and Automation*, 2013, 1574–1579.

[8] J. Mahler, et al., "Energy-bounded caging : formal definition and 2-D energy lower bound algorithm based on weighted alpha shapes," *IEEE Robotics and Automation Letters*, 1, 1, 508–515, 2016.

[9] Y. Jiang, et al., "Learning to place new objects," in *Proc. of IEEE Int. Conf. on Robotics and Automation*, 2012, 3088–3095.

[10] Y. Maeda, et al., "Analysis of indeterminate contact forces in robotic grasping and contact tasks," in *Proc. of IEEE/RSJ Int. Conf. on Intelligent Robots and Systems*, 2007, 1570–1575.

[11] C. D. Mladenova, "Group theory in the problems of modeling and control of multi-body systems," *J. of Geometry and Symmetry in Physics*, 8, 17–121, 2006.

[12] S. Makita and Y. Maeda, "Joint torque optimization for quasi-static graspless manipulation," in *Proc. of IEEE Int. Conf. on Robotics and Automation*, 2013, 3715–3720.

[13] T. Omata and K. Nagata, "Rigid body analysis of the indeterminate grasp force in power grasps," *IEEE Trans. on Robotics and Automation*, 16, 1, 46–54, February 2000.

[14] T. Omata, "Rigid body analysis of power grasps: Bounds of the indeterminate grasp force," in *Proc. of IEEE Int. Conf. on Robotics and Automation*, 2001, 2203–2209.

[15] P. J. Blau, *Friction Science and Technology*, 1st ed. CRC Press, 1996.

[16] Y. Maeda and S. Makita, "A quantitative test for the robustness of graspless manipulation," in *Proc. of IEEE Int. Conf. on Robotics and Automation*, 2006, 1743–1748.